

# VIKSER: Visual Knowledge-Driven Self-Reinforcing Reasoning Framework

Chunbai Zhang<sup>1,2</sup> Chao Wang<sup>1,2†</sup> Yang Zhou<sup>3†</sup> Yan Peng<sup>1,2</sup>

## Abstract

Visual reasoning refers to the task of solving questions about visual information. Current visual reasoning methods typically employ pre-trained vision-language model (VLM) strategies or deep neural network approaches. However, existing efforts are constrained by limited reasoning interpretability, while hindered by the phenomenon of underspecification in the question text. Additionally, the absence of fine-grained visual knowledge limits the precise understanding of subject behavior in visual reasoning tasks. To address these issues, we propose VIKSER (Visual Knowledge-Driven Self-Reinforcing Reasoning Framework). Specifically, VIKSER, trained using knowledge distilled from large language models, extracts fine-grained visual knowledge with the assistance of visual relationship detection techniques. Subsequently, VIKSER utilizes fine-grained visual knowledge to paraphrase the question with underspecification. Additionally, we design a novel prompting method called Chain-of-Evidence (CoE), which leverages the power of “evidence for reasoning” to endow VIKSER with interpretable reasoning capabilities. Meanwhile, the integration of self-reflection technology empowers VIKSER with the ability to learn and improve from its mistakes. Experiments conducted on widely used datasets demonstrate that VIKSER achieves new state-of-the-art (SOTA) results in relevant tasks.

## 1. Introduction

Endowing machines with robust logical reasoning capabilities has been a long-standing goal of vision-language models (VLMs) (Steiner et al., 2024; Liu et al., 2023b;

<sup>†</sup>Corresponding author <sup>1</sup>School of Future Technology, Shanghai University, Shanghai, 200444, China. <sup>2</sup>Institute of Artificial Intelligence, Shanghai University, Shanghai, 200444, China. <sup>3</sup>School of Mechatronic Engineering and Automation, Shanghai, 200444, China. Correspondence to: Chao Wang <cwang@shu.edu.cn>, Yang Zhou <saber\_mio@shu.edu.cn>.

Under review.

Kamath et al., 2021). A critical step toward realizing the goal lies in enhancing the model’s visual reasoning capabilities (Wu et al., 2024; Ray et al., 2024). Visual reasoning involves solving questions about visual information (Gupta & Kembhavi, 2023; He et al., 2021), a task that necessitates precise alignment between visual and textual features, along with advanced logical reasoning skills (Chang et al., 2024; Prasad et al., 2024; Zhang et al., 2023). Figure 1 illustrates a typical example of visual reasoning, where an agent must accurately align the image with the question and infer the intent through multiple steps of logical reasoning. The notable features of visual reasoning not only drive advancements in cross-modal learning (Deitke et al., 2024; Bazi et al., 2023) but also contribute to enhancing machines’ logical reasoning abilities (Prasad et al., 2024; Marcu et al., 2024), underscoring its substantial research significance.

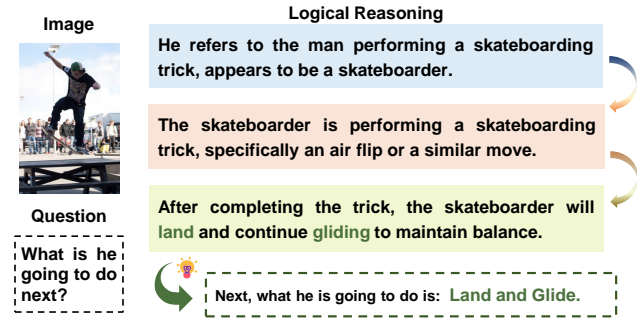


Figure 1. A typical example of visual reasoning. This complex task requires an agent to accurately align the image with the question and infer the intent through multi-step logical reasoning.

Existing visual reasoning methods typically employ pre-trained VLM strategies or deep neural network frameworks (Steiner et al., 2024; Deitke et al., 2024; Zakari et al., 2022). However, the reasoning capabilities of current efforts still exhibit limited interpretability (i.e., **Issue 1**). Additionally, underspecification is a common phenomenon in visual reasoning tasks (Prasad et al., 2024; Pezzelle, 2023), where an ambiguous description of the subject in the question text can hinder the alignment between textual and visual features, leading to multiple incorrect visual interpretations and undermining reasoning reliability (i.e., **Issue 2**). As shown in Figure 1, the subject “he” in the question is ambiguously described, which may be confused with other individuals in the image, presenting a risk of incorrect reasoning. On

the other hand, visual knowledge extraction (VKE) techniques, which provide enriched visual information, have the potential to significantly assist in addressing visual reasoning tasks (Cui et al., 2024; Yang et al., 2024a). However, *existing VKE methods are insufficient in extracting latent and fine-grained visual knowledge* (i.e., **Issue 3**). The issue limits the accurate understanding of subject behavior in complex questions, thereby hindering the interpretability and precision required for visual reasoning tasks.

To address these issues, we design VIKSER (**Visual Knowledge-Driven Self-Reinforcing Reasoning Framework**). The core components of VIKSER are the fine-grained visual knowledge extraction ( $F$ -VKE) module and the self-reinforcing reasoning ( $S$ -RR) module. For **Issue 1**, we deploy the  $S$ -RR module, which offers enhanced interpretability in reasoning and integrates self-reinforcement capabilities. Specifically, the module integrates a novel prompting technique, Chain-of-Evidence (CoE), which we propose to enhance interpretability by facilitating step-by-step reasoning grounded in factual evidence. Meanwhile, a self-reflection mechanism, which utilizes insights from past failures to refine future reasoning, is introduced to facilitate adaptive reinforcement. Additionally, intending to address **Issue 2**, a specification paraphrase method is explored for the  $S$ -RR module. Concretely, we collect object-level information from fine-grained visual knowledge to refine ambiguous descriptions of the subject in question, thereby improving the question’s clarity and completeness.

To address **Issue 3**, we deploy the  $F$ -VKE module to provide fine-grained visual knowledge to VIKSER. To be specific, the  $F$ -VKE module first detects the detailed visual relationships among key entities in an input image. Subsequently, we train the  $F$ -VKE module using knowledge distilled from large language models (LLMs) to uncover causal relationships between entities’ behaviors and their inferred outcomes. For instance, as shown in Figure 3, LLMs can infer that a man depicted squatting on the right side of the train door may disembark at the next station. Following this, the trained  $F$ -VKE module leverages visual and causal relationships to generate fine-grained visual knowledge. A specific case that validates the fine-grained nature and richness of the visual knowledge generated by the  $F$ -VKE module is provided in Section 4.4. We conduct extensive experiments on diverse widely-recognized datasets to validate VIKSER’s visual knowledge extraction and reasoning capabilities. The results demonstrate that VIKSER outperforms the latest research across all datasets, achieving new SOTA results.

We summarize our **contributions** as follows:

- We propose VIKSER, a novel framework for visual reasoning tasks, which extracts fine-grained and enriched visual knowledge while performing highly interpretable and self-reinforcing reasoning.

- A specification paraphrase method is designed to help VIKSER mitigate underspecification, while a novel CoE prompting technique and a self-reflection mechanism are introduced to assist VIKSER in performing highly interpretable and self-reinforcing reasoning.
- Extensive experimental results demonstrate VIKSER’s improvements over advanced baselines across diverse public datasets, achieving new SOTA results.

## 2. Related Work

**Visual Knowledge Extraction** Existing VKE methods either employ a holistic image captioning strategy or rely on fixed knowledge formats to extract visual information (Cui et al., 2023; Liu et al., 2023b). Specifically, deep learning has played a crucial role in advancing image captioning approaches (Jiang et al., 2018; Yao et al., 2017). With the development of VLMs, an increasing number of studies leverage pre-trained multimodal large language models (MLLMs) to understand both visual and textual information in a unified framework (Hu et al., 2023; Fang et al., 2022). On the other hand, the image captioning methods provide a broad understanding of the image content, yet they encounter challenges in conveying fine-grained details. In contrast, some studies utilize fixed knowledge graphs to map visual features to predefined semantic categories (Yang et al., 2024a; Li et al., 2023b), providing a structured form of visual knowledge (Li et al., 2024; Zareian et al., 2020). While these methods ensure consistency and interpretability, they fall short in providing enriched visual knowledge.

**Language Model Reasoning** Recently, large VLMs have demonstrated remarkable success in reasoning and inference, particularly in facilitating few-shot (Lang et al., 2022; Gao et al., 2021) and zero-shot (Yu et al., 2024; Kojima et al., 2022) learning. Meanwhile, the potential of prompt-based reasoning has been extensively explored to tackle diverse cross-modal visual reasoning tasks, including visual question answering (VQA) (Prasad et al., 2024; Wu et al., 2024), visual entailment (VE) (Kayser et al., 2021), and visual commonsense reasoning (VCR) (Chang et al., 2024; Sammani et al., 2022). By leveraging the substantial information embedded within VLMs, novel insights are generated to advance reasoning and interpretability research.

## 3. Method

In this section, we provide detailed descriptions of VIKSER’s  $F$ -VKE module and  $S$ -RR module. Specifically, the  $F$ -VKE module consists of two agents: the visual relationship detector ( $Ag$ -VRD) and the visual knowledge enRicher ( $Ag$ -VKR), where  $Ag$ -VKR consists of a causal relationship analyzer  $G_a$  and an image caption generator  $G_c$ .

Starting with the input image  $I$  and question  $Q$ ,  $Ag\text{-VRD}$  first detects the visual relationships between key entities in  $I$  and integrates these relationships into a preliminary visual description  $D$ . Following this,  $G_a$  in  $Ag\text{-VKR}$  provides an analysis report  $A$  of the causal relationships between key entities’ behaviors in  $D$  and their inferred outcomes. For instance, a description of a man squatting at the train door implicitly suggests that he may disembark at the next station. Finally, leveraging  $A$ ,  $G_c$  in  $Ag\text{-VKR}$  enriches  $D$  into a more detailed and nuanced image caption  $C$ , offering fine-grained visual knowledge. On the other hand, the  $S\text{-RR}$  module is composed of the specification paraphraser ( $Ag\text{-SPR}$ ) and the self-refining reasoner ( $Ag\text{-SR}$ ). Specifically,  $Ag\text{-SPR}$  first collects visual information from  $C$  to refine ambiguous descriptions of the subject in  $Q$ , thereby forming the paraphrased question  $Q_r$ . Subsequently,  $Ag\text{-SR}$  employs CoE prompting to infer the predicted answer  $\tilde{a}$  based on  $Q_r$ ,  $I$ , and  $C$ . When  $\tilde{a}$  exhibits positivity, it directly serves as the final answer  $a$ . Conversely, if  $\tilde{a}$  shows negativity,  $Ag\text{-SR}$  will use  $\tilde{a}$  and the reasoning trajectory  $t$  to perform self-reflection in search of a more valuable response. Figure 2 illustrates a detailed framework of VIKSER. Next, we will provide a detailed introduction to the modules of VIKSER.

### 3.1. Fine-Grained Visual Knowledge Extraction

Guided by the principles of multi-agent collaboration, the functionality of the  $F\text{-VKE}$  module in extracting fine-grained visual knowledge is distributed across two agents: the visual relationship detector  $Ag\text{-VRD}$  and the visual knowledge enricher  $Ag\text{-VKR}$ . The architectural design of  $Ag\text{-VRD}$  and the  $Ag\text{-VKR}$  is elaborated as follows.

**Visual Relationship Detector** Accurate detection of entities in images and their relationships form the foundation for effective VKE techniques. With the aim of endowing the  $F\text{-VKE}$  module with efficient visual relationship detection capabilities, we design the  $Ag\text{-VRD}$  based on existing VRD methods. Concretely, given an input image  $I$ , the  $Ag\text{-VRD}$  is prompted to extract all entities within the image. Each entity is then assigned a validity score  $S_e$ , reflecting its relevance in understanding the image’s content. Notably, when the entity’s score exceeds a predefined threshold  $\theta_e$ , it is classified as a key entity  $K_e$ . Following this, with the aid of CoVLM (Li et al., 2024), we extract all relevant visual relationships of  $K_e$ . CoVLM is an exceptional VRD method that facilitates the collaboration between visual detection networks and LLMs, utilizing specially designed communication tokens. The advantage of CoVLM lies in its ability to precisely identify the target entity  $E_B$  corresponding to a given relationship based on the input entity  $E_A$ , by leveraging the specially crafted communication tokens. However, due to the fixed structure of its communication tokens, CoVLM is limited in offering fine-grained visual

knowledge. Therefore, we utilize CoVLM primarily for refining the detected visual relationships.

To be specific, we first employ the detection network of CoVLM to identify the regions of interest corresponding to each  $K_e$  in  $I$ . Based on these regions and their associated entities, the  $Ag\text{-VRD}$  is then prompted to detect all potential relationships associated with  $K_e$ . Subsequently, we employ CoVLM to detect the relevant entities corresponding to these potential relationships. These potential relationships are then merged with their associated entities to form the visual relationship  $r$ . Following this, the  $Ag\text{-VRD}$  is employed to assess a relationship validity score  $S_r$  for each  $r$  based on its effectiveness in contributing to the understanding of  $I$ . To determine which visual relationships associated with the key entities are truly effective in capturing the semantics of the input image, we propose a joint entity-relation validity evaluation algorithm to compute the entity-relation joint validity score  $S_r^e$ :

$$S_r^e = S_e \cdot \omega_r \cdot S_r, \omega_r = 1 + \gamma(\alpha - N_r^e), \quad (1)$$

where  $S_e$  denotes the entity validity score and  $S_r$  denotes the relationship validity score.  $\omega_r$  represents the weight associated with the current visual relationship  $r$ .  $N_r^e$  denotes the number of  $r$  held by the key entity  $K_e$ .  $\gamma$  and  $\alpha$  are hyperparameters, where  $\gamma$  controls the influence of the number of visual relationships on the weight, constrained within the range (0.05, 0.2). And  $\alpha$  limits the number of visual relationships. For example, as  $N_r^e$  increases,  $\omega_r$  decreases to amplify the constraint of  $S_r^e$  on the visual relationship. Conversely,  $\omega_r$  increases when the number of relationships is smaller. Additionally, in case  $S_r^e$  exceeds a threshold  $\theta_r^e$ , the corresponding visual relationship under the current key entity is labeled as a key visual relationship  $K_r$ . After identifying  $K_e$  and  $K_r$ , we generate the preliminary image description  $D$  by progressively aligning each  $K_e$  with its corresponding  $K_r$ .

**Visual Knowledge Enricher** Existing VRD methods primarily focus on detecting surface-level, concept-based relational information within an image (Li et al., 2024; Yang et al., 2024b). This nature makes it challenging for current VRD methods to conduct in-depth, object-level analysis of the image content. However, such analyses are essential for a comprehensive understanding of the image. For this reason, we further deploy  $Ag\text{-VKR}$ , which consists of a causal relationship analyzer  $G_a$  and an image caption generator  $G_c$ , to enhance the depth of knowledge in image analysis. Specifically,  $G_a$  first interprets the preliminary image description  $D$  concerning the input image  $I$ . Next,  $G_a$  derives an analysis report  $A$  that uncovers the causal relationships between the behaviors of key entities in  $D$  and their inferred outcomes. Subsequently,  $G_c$  enriches  $D$  by incorporating the visual knowledge from  $I$  and  $A$ , resulting in a detailed image caption  $C$  for  $I$ .

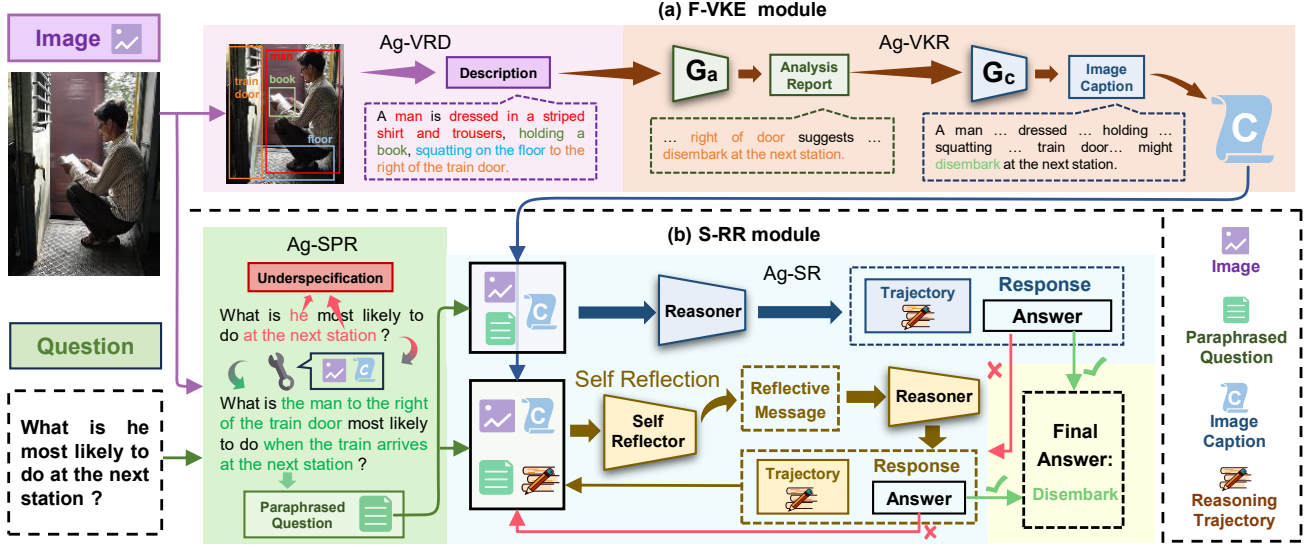


Figure 2. The framework of VIKSER. Starting with the input image and question, VIKSER first extracts the relationships between key entities in the image and analyzes these relationships to form a detailed image caption. Then, VIKSER uses the image caption to paraphrase the question, refining the ambiguous descriptions in the question. Finally, VIKSER infers a predicted answer based on the paraphrased question, the image, and its caption. The predicted answer is taken as the final answer if it sufficiently addresses the question. Otherwise, VIKSER performs self-reflection based on the reasoning trajectory, the paraphrased question, the image, and its caption to seek a more valuable response.

Causal relationship analysis reporting and detailed image captioning typically require training with ground-truth data, which is often absent in existing datasets. To address this, we propose leveraging the extensive knowledge reservoir inherent in LLMs (e.g., ChatGPT-4 (Achiam et al., 2023)) to generate causal relationship analysis reports and detailed image captions as pseudo-ground-truth data to train  $G_a$  and  $G_c$ . Specifically, we extract pseudo-ground-truth causal relationship analysis report  $A_p$  from LLM with a task-specific set of few-shot demonstrations as follows:

$$KA_p = \{A_p \mid A_p \sim P_{LLM}(I, D)\}, \quad (2)$$

where  $I$  denotes the input image,  $D$  represents the ground-truth preliminary image description of  $I$ , and  $P_{LLM}$  denotes the LLM operating in an autoregressive manner.  $A_p$  represents the pseudo-ground-truth causal relationship analysis report sampled from  $P_{LLM}$ , and  $KA_p$  represents the set of all  $A_p$ . However,  $KA_p$  may be noisy and erroneous, which could adversely affect the subsequent detailed image captioning process. To address this, we apply a post-processing mechanism to filter  $KA_p$  into  $KA'_p$ . Specifically, for each  $A_p$  in  $KA_p$ , we use a pre-trained MLLM (denoted as  $F$ ) to assess its validity score  $S_{A_p}$  based on whether  $A_p$  correctly uncovers the causal relationship. In case  $S_{A_p}$  exceeds a pre-determined threshold  $\tau$ , the corresponding  $A_p$  is retained. The process of collecting  $KA'_p$  is formalized as follows:

$$KA'_p = \{A_p \mid S_{A_p} > \tau\}, S_{A_p} = F(A_p, (I, D)), \quad (3)$$

where  $A_p$  denotes the pseudo-ground-truth causal relationship analysis report.  $I$  denotes the input image,  $D$  represents the ground-truth preliminary image description of  $I$ .  $\tau$  denotes the pre-determined threshold.  $F$  denotes the pre-trained MLLM. With  $KA'_p$  serving as pseudo-ground-truth data, we are able to train  $G_a$  with the distillation loss  $L_{G_a}$ , as formalized below:

$$L_{G_a} = - \sum_{t=1}^T \log(P_{G_a}(A'_{p,t} \mid A'_{p,t-1}, (I, D))), \quad (4)$$

where  $A'_p \in KA'_p$ , and  $T = |A'_p|$ . Figure 3 shows how we utilize knowledge distillation from the LLM to train  $G_a$ . Specifically, for the Image and Description, a post-processing mechanism employs  $F$  to determine whether  $S_{A_p}$  is passing, thereby filtering out the noise from the LLM-generated  $A_p$  to obtain  $A'_p$ . Following this,  $A'_p$  is used to train  $G_a$  via  $L_{G_a}$ , in order to generate  $A$ .

Similarly, we employ the same knowledge distillation approach to train  $G_c$ . Concretely, we utilize  $KA'_p$  as input to help  $G_c$  enrich the preliminary image description  $D$ , thereby generating pseudo-ground-truth image captions  $KC'_p$ . Subsequently, we train the image caption generator  $G_c$  with the distillation loss  $L_{G_c}$  described below:

$$L_{G_c} = - \sum_{t=1}^T \log(P_{G_c}(C'_{p,t} \mid C'_{p,t-1}, (I, D, A'_p))), \quad (5)$$

where  $C'_p \in KC'_p$ ,  $A'_p \in KA'_p$ , and  $T = |C'_p|$ . More details

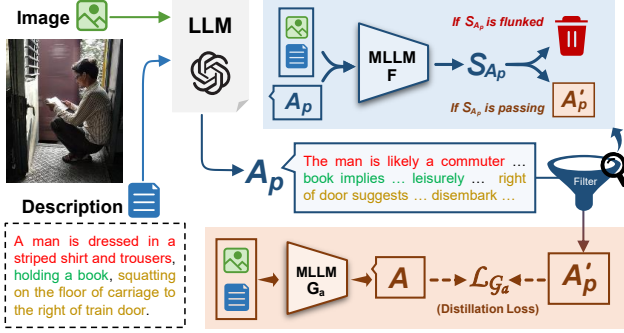


Figure 3. Process of utilizing knowledge distillation from LLM to train  $G_a$  to generate  $A$ .

are discussed in Appendix A.1. In summary, the trained causal relationship analyzer  $G_a$  and image caption generator  $G_c$  operate collaboratively to fulfill the functionality of  $Ag-VKR$ . Specifically, given an input image  $I$  and the preliminary image description  $D$ ,  $G_a$  and  $G_c$  generate a detailed image caption  $C$  for  $I$ .

### 3.2. Self-Reinforcing Reasoning

We leverage the detailed visual knowledge in the image caption  $C$ , which is generated by the  $F-VKE$  module, to enhance the performance of VIKSER in visual reasoning tasks, such as VQA and VE. To achieve this, we propose an  $S-RR$  module, consisting of a specification paraphraser  $Ag-SPR$  and a self-refining reasoner  $Ag-SR$ , to endow VIKSER with advanced reasoning capabilities. Specifically, starting with an image and a question,  $Ag-SPR$  extracts and analyzes the fine-grained visual knowledge in  $C$ , to refine ambiguous descriptions in the question and paraphrase it. Subsequently,  $Ag-SR$  resolves the paraphrased question by leveraging the input image and the detailed image caption through a self-reinforcing reasoning paradigm. It is important to emphasize that we aim to develop a reasoning approach characterized by high generalizability and a gradient-free, in light of the diversity of visual reasoning tasks. For this reason, we propose employing a flexible and plug-and-play reasoning prompt paradigm to prompt pre-trained visual language models (PVLMs) to perform the functions of  $Ag-SPR$  and  $Ag-SR$ . Detailed prompts are discussed in Appendix A.2. The architectural design of  $Ag-SPR$  and the  $Ag-SR$  is elaborated as follows.

**Specification Paraphraser** Starting with the input image  $I$ , the original question  $Q$ , and the detailed image caption  $C$  generated by the  $F-VKE$  module,  $Ag-SPR$  leverages the detailed visual information in  $C$  to paraphrase  $Q$ , thereby refining any ambiguous descriptions within  $Q$ . We employ a PVLm as the core of  $Ag-SPR$  to facilitate this process. Specifically, we prompt the PVLm in  $Ag-SPR$  to first identify the main subject in  $Q$ , and then query  $C$  for relevant

textual information. Meanwhile, the PVLm is prompted to extract the interaction between the main subject and the image scene from  $C$ , providing a complementary description of the main subject’s context. Subsequently, the above textual information is paraphrased in natural language and integrated into  $Q$  to form the paraphrased question  $Q_r$ . The underlying logic of this process is that the entities mentioned in  $Q$  intuitively provide key information relevant to the expected answer intuitively. For this reason, providing more detailed descriptions of the subject aids the  $S-RR$  module in resolving the visual reasoning task.

**Self-Refining Reasoner** As a key component of the  $S-RR$  module, the cognitive and reasoning capabilities of  $Ag-SR$  significantly influence the overall problem-solving performance of the system. To enhance  $Ag-SR$ ’s capabilities, we introduce a prompting technique called CoE, which guides  $Ag-SR$  to reason incrementally and provide highly interpretable steps toward the expected answer of  $Q_r$ . Furthermore, we present a self-reflection mechanism that allows  $Ag-SR$  to perform self-correction, thereby improving its robustness in reasoning. Detailed descriptions are as follows.

*Highly Interpretable Reasoning:* We prompt a PVLm to serve as the core of  $Ag-SR$ . Given that conventional reasoning prompts, such as ”think step-by-step” (Wei et al., 2022), often induce hallucinations due to insufficiently grounded rationale, we propose CoE, a tailored prompting technique, to enhance the PVLm’s reasoning ability. Concretely, the PVLm first analyzes fine-grained visual knowledge provided by the  $F-VKE$  module, extracting factual information to serve as evidence for reasoning. Subsequently, CoE guides the PVLm through a structured, step-by-step reasoning process based on the extracted evidence, ultimately generating a predicted answer  $\tilde{a}$ . This reasoning framework enables CoE to enhance interpretability while improving reasoning accuracy. Further details on CoE prompting are provided in Appendix A.2.

*Self-Reflection-Based Reinforcement Mechanism:* Existing research has shown that even highly intelligent agents are susceptible to generating low-quality answers, which significantly diminishes the accuracy of their reasoning and decision-making processes. To address this, we propose a self-reflection mechanism that builds upon the method proposed by Shinn et al (Shinn et al., 2024). The mechanism enables  $Ag-SR$  to manage instances of low-quality answers by leveraging past experiences, thereby reducing the likelihood of similar errors occurring in the future. Specifically, after deriving  $\tilde{a}$ ,  $Ag-SR$  utilize an exact matching mechanism to map complex natural language information in  $\tilde{a}$  to a two-dimensional discrete binary reward score  $S_{ref}$ . If  $S_{ref}$  is positive, the predicted answer  $\tilde{a}$  is directly used as the final answer  $a$ . In contrast, when  $S_{ref}$  is represented as negative,  $Ag-SR$  is prompted to analyze  $Q_r$  and a reasoning

trajectory  $t$  from the previous trial. Subsequently,  $Ag$ -SR reflects on the cause of failure and generates a detailed verbal reflection, denoted as  $V_{ref}$ . Following this,  $V_{ref}$  serves as experiential knowledge to guide  $Ag$ -SR in generating a more accurate answer in subsequent trials. It is important to note that, compared to the reward score  $S_{ref}$ ,  $V_{ref}$  encompasses more comprehensive experiential information. For instance, while  $S_{ref}$  merely indicates success or failure,  $V_{ref}$  provides insight into which aspects of the previous reasoning trajectory were incorrectly applied, resulting in previous failure. Furthermore,  $V_{ref}$  can provide guidance on how to avoid similar mistakes in future trials.

## 4. Experiments

In this section, we conduct extensive experiments on publicly available datasets to evaluate VIKSER’s performance.

### 4.1. Experimental Setup

In our experiments, we prompt GPT-4o mini (OpenAI, 2024) as the LLM foundation for  $Ag$ -VRD of the  $F$ -VKE module in VIKSER. Additionally, we employ LLaVa-1.5-7B (Liu et al., 2023b) as the PVLm foundation for the  $S$ -RR module of VIKSER. It is important to note that in Section 3.1, the LLM used for knowledge distillation is ChatGPT-4 (Achiam et al., 2023), while  $G_a$  and  $G_c$  are obtained through training LLaVa-1.5-7B. On the other hand, a summary of the experimental setup is provided, which includes the datasets, baseline methods, and evaluation metrics employed for performance assessment.

**Datasets:** To evaluate the reasoning abilities of VIKSER, we utilize widely-used datasets for visual reasoning tasks, including VQAv2 (Goyal et al., 2017), A-OKVQA (Schwenk et al., 2022), VizWiz (Gurari et al., 2018), e-SNLI-VE (Kayser et al., 2021), CoLA (Ray et al., 2024), and CREPE (Ma et al., 2023).

**Baselines:** We compare VIKSER with 12 competitive baselines, including SMOla-PaLI-X (Wu et al., 2024), LLaVa-1.5-7B (Liu et al., 2023b), REPARE (Prasad et al., 2024), CoVLM (Li et al., 2024), Molmo-72B (Deitke et al., 2024), PaLi-X (Chen et al., 2022), PaliGemma 2 (Steiner et al., 2024), NLX-GPT (Sammani et al., 2022), Rapper (Chang et al., 2024), e-UG (Kayser et al., 2021), OFX-X (Plüster et al., 2022), MosaiCLIP (Singh et al., 2023), CLIP+ MM-Pred (Ray et al., 2024), and CLIP+ Linear (Ray et al., 2024).

**Evaluation Metrics:** Based on previous work (Ray et al., 2024; Ma et al., 2023; Prasad et al., 2024; Chang et al., 2024), we adopt appropriate dataset-specific metrics for evaluation. Specifically, (1) For the VQAv2 dataset, we evaluate accuracy separately for the yes/no (Y/N), number (Num.), and other (Other) types of questions, and additionally evaluate overall accuracy (Overall). (2) For the

A-OKVQA dataset, we evaluate both Direct Answer accuracy (DA.) and Multiple Choice accuracy (MC.). (3) For the VizWiz dataset, we evaluate overall accuracy (Overall). (4) For the Cola, CREPE, and e-SNLI-VE datasets, we assess Accuracy (Acc.). Notably, for the CREPE dataset, we further evaluate Recall@1 (R@1).

### 4.2. Main Results

We conduct extensive experiments to validate VIKSER’s visual reasoning capabilities, with the main experimental results summarized as follows.

**VIKSER performs outstandingly in reasoning and answering visual questions.** To validate the superiority of VIKSER’s visual reasoning capabilities, we compare its performance with eight competitive baselines on the VQAv2, A-OKVQA, and VizWiz datasets, as presented in Table 1. To be specific, VIKSER achieves new SOTA results across all datasets, with the exception of the Num. metric on the VQAv2 dataset. Notably, when LLaVa-1.5-7B is used as the PVLm foundation for the  $S$ -RR module, VIKSER significantly outperforms LLaVa-1.5-7B across all metrics. In particular, on the MC. metric of the A-OKVQA dataset, VIKSER achieves an almost 30% improvement over LLaVa-1.5-7B. Meanwhile, VIKSER, employing a gradient-free reasoning paradigm, continues to outperform task-specific methods pre-trained on the datasets. These substantial advantages demonstrate the superiority and generalizability of VIKSER’s reasoning paradigm. Moreover, VIKSER, with fewer parameters, outperforms baselines with more parameters, such as Molmo-72B and PaliGemma-2 (10B), across all metrics except for Num. The advancements highlight VIKSER’s potential in visual reasoning tasks.

On the other hand, we analyze the reasons for VIKSER’s slight underperformance on the Num. metric of the VQAv2 dataset as follows: (1) VIKSER has fewer model parameters, larger models, such as Molmo-72B, benefit from a larger parameter size; (2) VIKSER prioritizes extracting information from key entities in the image, which may lead to a potential risk of overlooking a holistic analysis of the image. For these reasons, VIKSER performs slightly worse on visual reasoning tasks involving numerical questions compared to more powerful LLMs, such as Molmo-72B. Nonetheless, we believe there is still room for improvement in VIKSER’s numerical analysis performance.

**VIKSER performs excellently in reasoning and understanding visual information.** To further evaluate the reasoning performance of VIKSER, we compare it with nine competitive baselines on the Cola, CREPE, and e-SNLI-VE dataset, as shown in Table 2 and Figure 4. Specifically, VIKSER outperforms existing methods, achieving a new SOTA result. It is worth noting that both the Cola and CREPE datasets require a model to precisely match images

Table 1. Comparative performance of different methods on the VQAv2, A-OKVQA, and VizWiz datasets.   represents the optimal scores, while   represents the suboptimal scores. We replicate the scores of LLaVa-1.5-7B and CoVLM, while the scores for the remaining baselines are sourced from the official repositories of VQAv2, A-OKVQA, and VizWiz datasets, as well as the study conducted by Prasad et al. (Prasad et al., 2024).

METHODS	VQAv2				A-OKVQA		VizWiz
	OVERALL (%)	Y/N (%)	NUM. (%)	OTHER (%)	MC. (%)	DA. (%)	OVERALL (%)
GENERAL METHODS							
LLAVA-1.5-7B	74.04	86.84	52.94	57.89	62.56	77.38	57.07
REPAIRE + LLAVA-1.5	77.34	92.64	59.92	70.12	66.19	<span style="background-color: #fff2cc;">78.21</span>	59.46
REPAIRE + BLIP-2	74.05	94.56	54.40	63.36	55.67	82.80	70.03
MOLMO-72B	86.67	96.91	<span style="background-color: #d9ead3;">78.49</span>	79.63	82.20	74.95	-
VRD METHODS							
CoVLM	48.80	64.02	36.85	40.37	46.47	52.35	44.32
TASK-SPECIFIC METHODS							
SMOLA-PALI-X	85.00	-	-	-	<span style="background-color: #fff2cc;">84.1</span>	70.55	72.00
PALI-X	86.06	96.78	74.14	79.46	80.4	68.20	73.30
PALI-GEMMA 2	<span style="background-color: #fff2cc;">86.95</span>	<span style="background-color: #fff2cc;">97.19</span>	77.77	<span style="background-color: #fff2cc;">80.13</span>	83.7	71.30	<span style="background-color: #fff2cc;">78.10</span>
VIKSER (OURS)	<span style="background-color: #d9ead3;">88.74</span>	<span style="background-color: #d9ead3;">98.31</span>	<span style="background-color: #fff2cc;">75.51</span>	<span style="background-color: #d9ead3;">86.71</span>	<span style="background-color: #d9ead3;">92.51</span>	<span style="background-color: #d9ead3;">88.53</span>	<span style="background-color: #d9ead3;">82.52</span>

with captions. Therefore, the success of VIKSER highlights its capacity to accurately interpret image content and effectively extract information from key entities, enabling it to perform visual reasoning tasks with high precision.

Table 2. Comparative performance of different methods on the Cola and CREPE datasets. The baseline scores are sourced from related studies (Li et al., 2024; Ray et al., 2024).

METHODS	COLA		CREPE	
	ACC. (%)	ACC. (%)	R@1 (%)	
MOSAICLIP	-	-	<span style="background-color: #fff2cc;">90.2</span>	
CLIP + MM-PRED	41.42	77.84	-	
CLIP + LINEAR	30.47	<span style="background-color: #fff2cc;">87.35</span>	-	
CoVLM	<span style="background-color: #fff2cc;">44.29</span>	-	-	
VIKSER (OURS)	<span style="background-color: #d9ead3;">49.49</span>	<span style="background-color: #d9ead3;">96.68</span>	<span style="background-color: #d9ead3;">93.81</span>	

Additionally, as demonstrated in Figure 4, VIKSER performs outstandingly on the e-SNLI-VE dataset. Notably, VIKSER surpasses OFX-X by 8.72%, highlighting its effectiveness. The success of VIKSER underscores its ability to correctly infer the visual scene present in an image based on the visual information. We attribute this advantage to the seamless collaboration between the F-VKE and S-RR modules, as well as the flexible reasoning paradigm within the S-RR module. As discussed in Section 3.2, the plug-and-play nature and gradient-free design of the reasoning paradigm in the S-RR module endow VIKSER with high generalization capabilities, enabling it to adapt to diverse visual reasoning tasks.

### 4.3. Ablation Studies

We conduct various ablation experiments to evaluate the performance of each component of VIKSER. Specifically, on the VQAv2 dataset, we systematically ablate the *Ag-SPR*

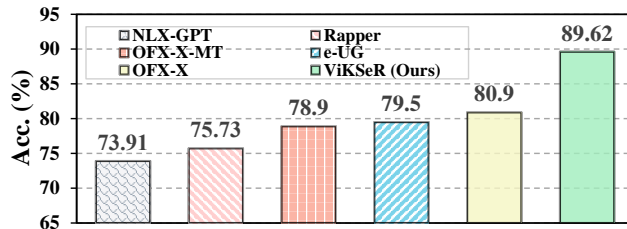


Figure 4. Comparative performance of different methods on the e-SNLI-VE dataset. The baseline scores are sourced from the official repository of e-SNLI-VE and the seminal study conducted by Chang et al. (Chang et al., 2024).

and self-reflection mechanism in the S-RR module to assess their impact on the performance of VIKSER. As shown in Table 3, on the VQAv2 dataset, ablating *Ag-SPR* individually results in the least impact on overall performance. In contrast, the simultaneous ablation of both *Ag-SPR* and the self-reflection mechanism leads to the most significant performance drop. Such findings suggest that both *Ag-SPR* and the self-reflection mechanism significantly contribute to the performance of VIKSER, with the self-reflection mechanism having a more substantial impact.

Table 3. Ablation results of experiments conducted on the VQAv2 and Cola datasets. W/O PARAPHRASER denotes the ablation of *Ag-SPR*, and W/O REFLECTION denotes the ablation of the self-reflection mechanism.

METHODS	VQAv2
	OVERALL (%)
VIKSER (OURS)	<span style="background-color: #d9ead3;">88.74</span>
W/O PARAPHRASER	81.68
W/O REFLECTION	77.86
W/O PARAPHRASER AND REFLECTION	74.04

On the other hand, to evaluate the capability of the  $F-VKE$  module, we conduct a qualitative analysis of the fine-grained visual knowledge extracted from two images. As shown in Figure 5, the  $F-VKE$  module precisely captures the fine-grained details within the images. Specifically, in the above image,  $F-VKE$  describes the boy’s appearance (e.g., “blonde hair” and “brown shirt”) and his physical actions (e.g., “standing” and “holding”). These valuable details contribute to a deeper comprehension of the image, facilitating the interpretation of its content by intelligent agents. Additionally,  $F-VKE$  further uncovers causal relationships embedded within the fine-grained details of the image (e.g., “he just took a bite of the pastry” and “the scene is taking place in colder weather”). The discovery suggests that  $F-VKE$  effectively learns the causal relationship uncovering capabilities of LLMs through the knowledge distillation process. Moreover,  $F-VKE$  also addresses additional aspects, such as the boy’s expressions (“curious” and “focused”), indicating that the boy is likely exploring the taste of the pastry. By linking these details to the action “took a bite of the pastry”,  $F-VKE$  constructs a more coherent causal pathway. Similarly, in the lower image,  $F-VKE$  accurately extracts fine-grained visual knowledge, including the man’s attire and physical actions, and further uncovers the underlying causal relationships (e.g., “he might disembark at the next station”). The fine-grained visual knowledge extracted by VIKSER’s  $F-VKE$  module includes detailed entity information as well as the causal relationships between entity behaviors and inferred outcomes, thereby offering significant assistance in solving related visual reasoning tasks.

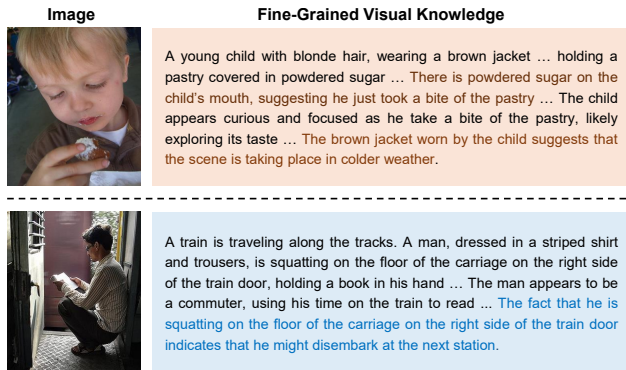


Figure 5. The fine-grained visual knowledge extracted by VIKSER from two images.

#### 4.4. Case Studies

To further validate the effectiveness of VIKSER, we conduct a qualitative analysis of its performance on two practical visual reasoning cases. As shown in Figure 6, in case (a), VIKSER identifies that the motorcyclist has a lit cigarette in his mouth while riding, by generating an image caption that contains fine-grained visual knowledge. This discovery serves as the foundation for solving the case (a). Subse-

quently, VIKSER utilizes the extracted visual knowledge to refine the ambiguous descriptions of the subject in the original question, resulting in a paraphrased question. Finally, through step-by-step reasoning with evidence, VIKSER infers the correct answer, “cigarette”. This practical visual reasoning case demonstrates VIKSER’s ability to extract fine-grained visual knowledge and its proficiency in utilizing visual facts as evidence for interpretable reasoning. Additionally, case (b) further demonstrates VIKSER’s self-reflection capability. Specifically, due to inevitable reasoning errors, VIKSER initially inferred an incorrect answer, “no”, in a previous reasoning process. Fortunately, with the assistance of the self-reflection mechanism, VIKSER generates a reflective message regarding its last failure, acknowledging that it had overlooked the fact that children may not pay attention to small details such as sugar on his faces while enjoying a treat. Subsequently, utilizing the reflective message, VIKSER accurately guides a new round of evidence-based reasoning and ultimately infers the correct answer, “yes”. This practical case demonstrates VIKSER’s ability to address reasoning errors through self-reflection and generate more valuable responses. More typical cases are discussed in Appendix A.3.

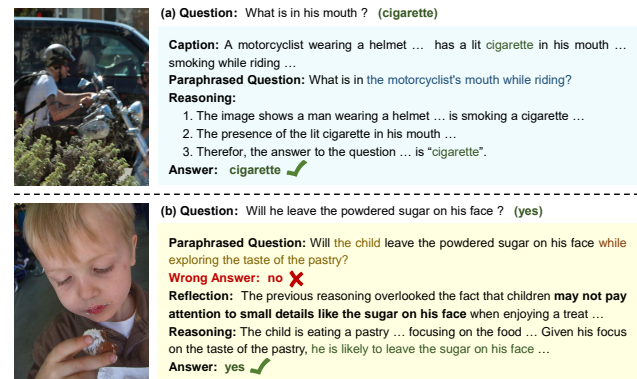


Figure 6. The performance of VIKSER on two practical visual reasoning cases.

## 5. Conclusion

In this paper, we introduce VIKSER, a new framework for visual reasoning tasks, which integrates the extraction of fine-grained and enriched visual knowledge with high interpretability and self-reinforcing reasoning capabilities. VIKSER comprises  $F-VKE$  and  $S-RR$  modules, as well as integrates advanced mechanisms to achieve superior performance. We conduct extensive experiments on diverse public datasets. The results demonstrate that VIKSER outperforms the latest research across public datasets, achieving new SOTA results. Our future work will focus on: 1) Exploring methods that extract finer-grained visual knowledge while performing more comprehensive visual reasoning based on overall image features. 2) Further integrating the capabilities of world models into VIKSER.

## References

- Achiam, J., Adler, S., Agarwal, S., Ahmad, L., Akkaya, I., Aleman, F. L., Almeida, D., Altenschmidt, J., Altman, S., Anadkat, S., et al. Gpt-4 technical report. *arXiv preprint arXiv:2303.08774*, 2023.
- Bai, J., Bai, S., Yang, S., Wang, S., Tan, S., Wang, P., Lin, J., Zhou, C., and Zhou, J. Qwen-vl: A versatile vision-language model for understanding, localization, text reading, and beyond. *arXiv preprint arXiv:2308.12966*, 2023.
- Bazi, Y., Rahhal, M. M. A., Bashmal, L., and Zuair, M. Vision-language model for visual question answering in medical imagery. *Bioengineering*, 10(3):380, 2023.
- Chang, K.-P., Huang, C.-P., Cheng, W.-Y., Yang, F.-E., Wang, C.-Y., Lai, Y.-H., and Wang, Y.-C. F. Rapper: Reinforced rationale-prompted paradigm for natural language explanation in visual question answering. In *Proceedings of the 2024 International Conference on Learning Representations (ICLR)*. OpenReview, 2024. URL <https://openreview.net/forum?id=bshfchPM9H>.
- Chen, X., Wang, X., Changpinyo, S., Piergiovanni, A., Padlewski, P., Salz, D., Goodman, S., Grycner, A., Mustafa, B., Beyer, L., et al. Pali: A jointly-scaled multilingual language-image model. *arXiv preprint arXiv:2209.06794*, 2022.
- Cui, H., Lin, R., Zalmout, N., Zhang, C., Shang, J., Yang, C., and Li, X. Pv2tea: Patching visual modality to textual-established information extraction. *arXiv preprint arXiv:2306.01016*, 2023.
- Cui, H., Fang, X., Zhang, Z., Xu, R., Kan, X., Liu, X., Yu, Y., Li, M., Song, Y., and Yang, C. Open visual knowledge extraction via relation-oriented multimodality model prompting. *Advances in Neural Information Processing Systems*, 36, 2024.
- Deitke, M., Clark, C., Lee, S., Tripathi, R., Yang, Y., Park, J. S., Salehi, M., Muennighoff, N., Lo, K., Soldaini, L., et al. Molmo and pixmo: Open weights and open data for state-of-the-art multimodal models. *arXiv preprint arXiv:2409.17146*, 2024.
- Fang, Z., Wang, J., Hu, X., Liang, L., Gan, Z., Wang, L., Yang, Y., and Liu, Z. Injecting semantic concepts into end-to-end image captioning. In *Proceedings of the IEEE/CVF Conference on Computer Vision and Pattern Recognition (CVPR)*, pp. 18009–18019, June 2022.
- Gao, T., Fisch, A., and Chen, D. Making pre-trained language models better few-shot learners. In Zong, C., Xia, F., Li, W., and Navigli, R. (eds.), *Proceedings of the 59th Annual Meeting of the Association for Computational Linguistics and the 11th International Joint Conference on Natural Language Processing (Volume 1: Long Papers)*, pp. 3816–3830, Online, August 2021. Association for Computational Linguistics. doi: 10.18653/v1/2021.acl-long.295. URL <https://aclanthology.org/2021.acl-long.295/>.
- Goyal, Y., Khot, T., Summers-Stay, D., Batra, D., and Parikh, D. Making the v in vqa matter: Elevating the role of image understanding in visual question answering. In *Proceedings of the IEEE conference on computer vision and pattern recognition*, pp. 6904–6913, 2017.
- Gupta, T. and Kembhavi, A. Visual programming: Compositional visual reasoning without training. In *Proceedings of the IEEE/CVF Conference on Computer Vision and Pattern Recognition (CVPR)*, pp. 14953–14962, June 2023.
- Gurari, D., Li, Q., Stangl, A. J., Guo, A., Lin, C., Grauman, K., Luo, J., and Bigham, J. P. Vizwiz grand challenge: Answering visual questions from blind people. In *Proceedings of the IEEE Conference on Computer Vision and Pattern Recognition (CVPR)*, June 2018.
- He, F., Wang, Y., Miao, X., and Sun, X. Interpretable visual reasoning: A survey. *Image and Vision Computing*, 112: 104194, 2021.
- Hu, Y., Hua, H., Yang, Z., Shi, W., Smith, N. A., and Luo, J. Promptcap: Prompt-guided image captioning for vqa with gpt-3. In *Proceedings of the IEEE/CVF International Conference on Computer Vision (ICCV)*, pp. 2963–2975, October 2023.
- Jiang, W., Ma, L., Jiang, Y.-G., Liu, W., and Zhang, T. Recurrent fusion network for image captioning. In *Proceedings of the European Conference on Computer Vision (ECCV)*, September 2018.
- Kamath, A., Singh, M., LeCun, Y., Synnaeve, G., Misra, I., and Carion, N. Mdetr-modulated detection for end-to-end multi-modal understanding. In *Proceedings of the IEEE/CVF international conference on computer vision*, pp. 1780–1790, 2021.
- Kayser, M., Camburu, O.-M., Salewski, L., Emde, C., Do, V., Akata, Z., and Lukasiewicz, T. e-vil: A dataset and benchmark for natural language explanations in vision-language tasks. In *Proceedings of the IEEE/CVF international conference on computer vision*, pp. 1244–1254, 2021.
- Kojima, T., Gu, S. S., Reid, M., Matsuo, Y., and Iwasawa, Y. Large language models are zero-shot reasoners. *Advances in neural information processing systems*, 35: 22199–22213, 2022.

- Lang, H., Agrawal, M. N., Kim, Y., and Sontag, D. Co-training improves prompt-based learning for large language models. In *International Conference on Machine Learning*, pp. 11985–12003. PMLR, 2022.
- Langley, P. Crafting papers on machine learning. In Langley, P. (ed.), *Proceedings of the 17th International Conference on Machine Learning (ICML 2000)*, pp. 1207–1216, Stanford, CA, 2000. Morgan Kaufmann.
- Li, J., Li, D., Savarese, S., and Hoi, S. Blip-2: Bootstrapping language-image pre-training with frozen image encoders and large language models. In *International conference on machine learning*, pp. 19730–19742. PMLR, 2023a.
- Li, J., Chen, D., Hong, Y., Chen, Z., Chen, P., Shen, Y., and Gan, C. Covlm: Composing visual entities and relationships in large language models via communicative decoding. In *The Twelfth International Conference on Learning Representations, ICLR 2024, Vienna, Austria, May 7-11, 2024*. OpenReview.net, 2024. URL <https://openreview.net/forum?id=PHGxChm115>.
- Li, Z., Zhu, X., Zhang, X., Zhang, Z., and Lei, Z. Visual commonsense based heterogeneous graph contrastive learning. *arXiv preprint arXiv:2311.06553*, 2023b.
- Liu, H., Li, C., Li, Y., and Lee, Y. J. Improved baselines with visual instruction tuning, 2023a.
- Liu, H., Li, C., Wu, Q., and Lee, Y. J. Visual instruction tuning, 2023b.
- Liu, H., Li, C., Li, Y., Li, B., Zhang, Y., Shen, S., and Lee, Y. J. Llava-next: Improved reasoning, ocr, and world knowledge, January 2024. URL <https://llava-vl.github.io/blog/2024-01-30-llava-next/>.
- Ma, Z., Hong, J., Gul, M. O., Gandhi, M., Gao, I., and Krishna, R. @ crepe: Can vision-language foundation models reason compositionally? In *Proceedings of the 2023 IEEE/CVF Conference on Computer Vision and Pattern Recognition*, pp. 10910–10921. IEEE, 2023. URL <https://doi.org/10.1109/CVPR52729.2023.01050>.
- Marcu, A.-M., Chen, L., Hünermann, J., Karnsund, A., Hanotte, B., Chidananda, P., Nair, S., Badrinarayanan, V., Kendall, A., Shotton, J., et al. Lingoqa: Visual question answering for autonomous driving. In *European Conference on Computer Vision*, pp. 252–269. Springer, 2024.
- OpenAI, G. 4o mini: Advancing cost-efficient intelligence, 2024. URL: <https://openai.com/index/gpt-4o-mini-advancing-cost-efficient-intelligence>, 2024.
- Pezzelle, S. Dealing with semantic underspecification in multimodal nlp. *arXiv preprint arXiv:2306.05240*, 2023.
- Plüster, B., Ambsdorf, J., Braach, L., Lee, J. H., and Wermter, S. Harnessing the power of multi-task pre-training for ground-truth level natural language explanations. *CoRR*, abs/2212.04231, 2022. URL <https://doi.org/10.48550/arXiv.2212.04231>.
- Prasad, A., Stengel-Eskin, E., and Bansal, M. Rephrase, augment, reason: Visual grounding of questions for vision-language models. In *The Twelfth International Conference on Learning Representations*, 2024. URL <https://openreview.net/forum?id=L4nOxziGf9>.
- Ray, A., Radenovic, F., Dubey, A., Plummer, B., Krishna, R., and Saenko, K. Cola: A benchmark for compositional text-to-image retrieval. *Advances in Neural Information Processing Systems*, 36, 2024.
- Sammani, F., Mukherjee, T., and Deligiannis, N. Nlx-gpt: A model for natural language explanations in vision and vision-language tasks. *CoRR*, abs/2203.05081, 2022. URL <https://doi.org/10.48550/arXiv.2203.05081>.
- Schwenk, D., Khandelwal, A., Clark, C., Marino, K., and Mottaghi, R. A-okvqa: A benchmark for visual question answering using world knowledge. In *European conference on computer vision*, pp. 146–162. Springer, 2022.
- Shinn, N., Cassano, F., Gopinath, A., Narasimhan, K., and Yao, S. Reflexion: Language agents with verbal reinforcement learning. *Advances in Neural Information Processing Systems*, 36, 2024.
- Singh, H., Zhang, P., Wang, Q., Wang, M., Xiong, W., Du, J., and Chen, Y. Coarse-to-fine contrastive learning in image-text-graph space for improved vision-language compositionality. *arXiv preprint arXiv:2305.13812*, 2023.
- Steiner, A., Pinto, A. S., Tschannen, M., Keysers, D., Wang, X., Bitton, Y., Gritsenko, A., Minderer, M., Sherbondy, A., Long, S., et al. Paligemma 2: A family of versatile vlms for transfer. *arXiv preprint arXiv:2412.03555*, 2024.
- Team, Q. Qwen2.5-vl, January 2025. URL <https://qwenlm.github.io/blog/qwen2.5-vl/>.
- Wang, P., Bai, S., Tan, S., Wang, S., Fan, Z., Bai, J., Chen, K., Liu, X., Wang, J., Ge, W., Fan, Y., Dang, K., Du, M., Ren, X., Men, R., Liu, D., Zhou, C., Zhou, J., and Lin, J. Qwen2-vl: Enhancing vision-language model’s perception of the world at any resolution. *arXiv preprint arXiv:2409.12191*, 2024.

- Wei, J., Wang, X., Schuurmans, D., Bosma, M., brian ichter, Xia, F., Chi, E. H., Le, Q. V., and Zhou, D. Chain of thought prompting elicits reasoning in large language models. In Oh, A. H., Agarwal, A., Belgrave, D., and Cho, K. (eds.), *Advances in Neural Information Processing Systems*, 2022. URL [https://openreview.net/forum?id=\\_VjQlMeSB\\_J](https://openreview.net/forum?id=_VjQlMeSB_J).
- Wu, J., Hu, X., Wang, Y., Pang, B., and Soricut, R. Omnismola: Boosting generalist multimodal models with soft mixture of low-rank experts. In *Proceedings of the IEEE/CVF Conference on Computer Vision and Pattern Recognition*, pp. 14205–14215, 2024.
- Yang, C., Xu, R., Guo, Y., Huang, P., Chen, Y., Ding, W., Wang, Z., and Zhou, H. Improving vision-and-language reasoning via spatial relations modeling. In *Proceedings of the IEEE/CVF Winter Conference on Applications of Computer Vision (WACV)*, pp. 769–778, January 2024a.
- Yang, C., Xu, R., Guo, Y., Huang, P., Chen, Y., Ding, W., Wang, Z., and Zhou, H. Improving vision-and-language reasoning via spatial relations modeling. In *Proceedings of the IEEE/CVF Winter Conference on Applications of Computer Vision (WACV)*, pp. 769–778, January 2024b.
- Yao, T., Pan, Y., Li, Y., Qiu, Z., and Mei, T. Boosting image captioning with attributes. In *Proceedings of the IEEE International Conference on Computer Vision (ICCV)*, Oct 2017.
- Yu, Y., Zhuang, Y., Zhang, J., Meng, Y., Ratner, A. J., Krishna, R., Shen, J., and Zhang, C. Large language model as attributed training data generator: A tale of diversity and bias. *Advances in Neural Information Processing Systems*, 36, 2024.
- Zakari, R. Y., Owusu, J. W., Wang, H., Qin, K., Lawal, Z. K., and Dong, Y. Vqa and visual reasoning: An overview of recent datasets, methods and challenges. *arXiv preprint arXiv:2212.13296*, 2022.
- Zareian, A., Karaman, S., and Chang, S.-F. Bridging knowledge graphs to generate scene graphs. In Vedaldi, A., Bischof, H., Brox, T., and Frahm, J.-M. (eds.), *Computer Vision – ECCV 2020*, pp. 606–623, Cham, 2020. Springer International Publishing. ISBN 978-3-030-58592-1.
- Zhang, Y., Chen, S., and Zhao, Q. Toward multi-granularity decision-making: Explicit visual reasoning with hierarchical knowledge. In *Proceedings of the IEEE/CVF International Conference on Computer Vision*, pp. 2573–2583, 2023.

## A. Appendix

### A.1. Training the Image Caption Generator

After obtaining the analysis reports  $KA'_p$ , the image caption generator  $G_c$  enriches the preliminary image description  $D$  by integrating the visual knowledge from the input image  $I$  and  $KA'_p$  to generate a detailed image caption  $C$  for  $I$ . As discussed in Section 3.1, we utilize profound-ground-truth data generated by the LLM to train the  $G_c$ . Specifically, we extract pseudo-ground-truth image caption  $C_p$  from LLM with a task-specific set of few-shot demonstrations as follows:

$$KC_p = \{C_p \mid C_p \sim P_{LLM}(I, D, A'_p)\}, \quad (6)$$

where  $I$  denotes the input image,  $D$  represents the ground-truth preliminary image description of  $I$ , and  $A'_p \in KA'_p$  represents the pseudo-ground-truth analysis report.  $P_{LLM}$  denotes the LLM operating autoregressively.  $C_p$  denotes the pseudo-ground-truth image caption sampled from  $P_{LLM}$ , and  $KC_p$  represents the set of all  $C_p$ .

Unfortunately,  $KC_p$  may contain noise and errors, adversely affecting the training of  $G_c$ . To address this, we similarly apply a post-processing mechanism to filter  $KA_p$  into  $KA'_p$ . Specifically, for each  $C_p$  in  $KC_p$ , we use  $F$  (the pre-trained MLLM) to assess its validity score  $S_{C_p}$  based on whether  $C_p$  correctly introduces the image. If  $S_{C_p}$  exceeds the predetermined threshold  $\tau$ , the corresponding  $C_p$  is retained. The process of collecting  $KC'_p$  is formalized as follows:

$$KC'_p = \{C_p \mid S_{C_p} > \tau\}, S_{C_p} = F(C_p, (I, D, A'_p)), \quad (7)$$

where  $C_p$  denotes the pseudo-ground-truth image caption.  $I$  denotes the input image,  $D$  represents the ground-truth preliminary image description.  $A'_p$  represents the pseudo-ground-truth analysis report.  $\tau$  denotes the predetermined threshold.  $F$  denotes the pre-trained MLLM. With  $KC'_p$  serving as pseudo-ground-truth data, we are able to train  $G_c$  with the distillation loss  $L_{G_c}$ , as formalized below:

$$L_{G_c} = - \sum_{t=1}^T \log(P_{G_c}(C'_{p,t} \mid C'_{p,t-1}, (I, D, A'_p))), \quad (8)$$

where  $C'_p \in KC'_p$ ,  $A'_p \in KA'_p$ , and  $T = |C'_p|$ . Finally, the trained  $G_c$  and  $G_a$  collaborate to generate a detailed image caption  $C$  for the input image  $I$ .

### A.2. Generating Reasoning from PVLMS

As discussed in Section 3.2, given the diversity of visual reasoning tasks, we propose a generalized, plug-and-play reasoning prompt paradigm to prompt PVLMS to activate the capacities of the S-RR module. In this section, we provide a detailed discussion of the design methodology for each prompt.

**Specification Paraphrase** After acquiring fine-grained visual knowledge from the F-VKE module, the S-RR module prompts a PVLMS to paraphrase the question text that exhibits underspecification. The prompt for specification paraphrasing is shown in Figure 7.

```
# You are an expert in question paraphrasing.
# You will be given an [Image], a [Question] about the [Image], and an [Image Caption].
# The [Question] about the [Image] may lack sufficient descriptions.
# Based on the [Image] and the [Image Caption], please supplement the ambiguous descriptions in the [Question].
...
# Note: The descriptions you need to supplement in the [Question] includes:
1. Descriptions of the main entity or subject mentioned in the [Question].
2. Descriptions of the background of the image and main subject that may not be mentioned in the [Question].
...
```

Figure 7. The prompt for paraphrasing the question text with underspecification.

**CoE Prompting** To answer the paraphrased question, the  $S$ -RR module employs CoE prompting to guide a PVLM in thinking step by step based on evidence and inferring a valuable response. As illustrated in Figure 8, CoE prompting first instructs the PVLM to leverage the visual information in the image and its caption to address the input question. Subsequently, the PVLM is encouraged to think step-by-step with evidence and generate both the answer and the step-by-step reasoning based on evidence. This reasoning framework helps the PVLM focus on the relevant visual information in the image and caption, using it as evidence to support interpretable reasoning.

```
# You are an expert in Visual Reasoning.
# Given an [Image], and a useful [Caption] about the [Image], as well as a [Question] about the [Image] to answer.
...
# Your task is to analyze the [Question], [Image] and [Caption] to construct a reasonable reasoning path to provide
an Answer to the [Question].
...
# Think step by step with evidence.
# Generate both [Answer] and [Step-by-step-reasoning-with-evidence].
...
# The format of your response is:
Step-by-step reasoning with evidence:[Your step-by-step-reasoning with evidence]
Answer: [Your Answer]
```

Figure 8. The prompt for the CoE prompting technique.

**Self Reflection** With the aim of addressing low-quality responses, the  $S$ -RR module prompts a PVLM to self-reflect on past failures and seek more valuable responses. As illustrated in Figure 9, the PVLM is tasked with analyzing the reasoning trajectory of past failures, reflecting on their causes, and formulating a high-level plan to prevent similar failures in the future. Finally, the PVLM will derive a more valuable answer based on the reflection information and the high-level plan.

```
# You are an advanced reasoning agent capable of improving based on self-reflection.
# You will be given the Result and [Trajectory] of a previous reasoning trial, where you were asked to answer a
[Question] but were unsuccessful in doing so.
...
# Based on the given [Image], [Question], and the [Trajectory] of the previous round of VQA reasoning, diagnose
the possible reason for failure or phrasing discrepancy in a few sentences, and devise a new, high-level plan to
mitigate similar failures. Please use complete sentences.
# Finally you should provide your Answer to the [Question] based on your Reflection.
...
```

Figure 9. The prompt for the self-reflection mechanism.

### A.3. Case studies

In this section, we demonstrate the capabilities of VIKSER on more typical visual reasoning cases. The baseline models selected for comparison include LLaVa 1.5, Qwen 2.5 (Bai et al., 2023), Blip2-Flan-T5-XXL (Li et al., 2023a), and GPT-4o-mini. It is worth noting that, due to the comparatively smaller parameter scales of LLaVa 1.5, Qwen 2.5, and Blip2-Flan-T5-XXL, we implement CoT prompting to augment their reasoning abilities. In contrast, for GPT-4o-mini, which possesses a substantially larger parameter size, we directly employ it for reasoning tasks without additional prompting strategies. Detailed results are shown in Figure 10, 11, 12 and 13. Specifically, Figure 10 and 11 compare the performance of VIKSER and the baselines on two visual reasoning tasks involving short-answer questions. While all baselines fail to solve both tasks, VIKSER excels by analyzing the fine-grained visual knowledge it extracts and applying correct reasoning to

answer the questions. Additionally, Figure 12 illustrates the performance of VIKSeR and the baseline models in addressing a visual reasoning task involving true/false questions. All baseline models fail to achieve satisfactory results in this task, especially Blip2-Flan-t5-xxl using CoT prompting, which fails to understand the question requirements and merely describes the image information in the answer. In contrast, VIKSeR demonstrates exceptional performance, successfully solving the visual reasoning task with remarkable accuracy and proficiency. Finally, Figure 13 presents the performance of VIKSeR and the baseline models in addressing a visual reasoning task involving short-answer questions. With the exception of GPT-4o-mini, all baseline models fail to achieve satisfactory results in this task. Notably, VIKSeR initially produces an incorrect result during the first round of reasoning. Fortunately, leveraging the self-reflection mechanism, VIKSeR identifies its mistake and re-infers the correct answer.



**Question:**  
What type of fruit is cut in half and darker than the other?

**Answer:**  
grapes.

**Reasoning:** Llava 1.5 - CoT  
The image shows a plate of food with a fork and a knife on it. The fork is silver and has a handle. The plate contains a salad with various vegetables, including tomatoes and carrots. The darker fruit is the tomato.  
**Final Answer:** Tomato. ❌

**Reasoning:** Qwen2.5 - CoT  
The image shows a plate of food consisting of a piece of meat, mushrooms, and a salad with various vegetables and a creamy dressing. There are no fruits visible in the image. The question asks about a fruit that is cut in half and darker than the others, it is not possible to identify any fruit based on the given image.  
**Final Answer:** There is no fruit. ❌

**Reasoning:** Blip2-Flan-t5-xxl - CoT  
Based on the image, we can see several fruits on the plate. Upon closer inspection, one fruit is cut in half, with its flesh clearly exposed. This cut fruit appears darker than the others, with a deep green color. Considering this color and texture, it is inferred that this fruit is a kiwi. Therefore, The fruit is a kiwi fruit.  
**Final Answer:** kiwi. ❌

**Reasoning:** GPT-4o-mini  
The fruit you are referring to could be an avocado. When an avocado is cut in half, the inside is typically a lighter green or yellow color, while the outer skin is darker, especially when the fruit is ripe. The flesh of the avocado is soft and creamy, with a large round pit in the center that needs to be carefully removed.  
**Final Answer:** avocado. ❌

**Caption:** VIKSeR (Ours)  
A appealing plate of salad features a chicken breast cut into bite-sized pieces ... The salad contains an array of **cut vegetables and fruits**, including **grapes**, lettuce and mushrooms ... adding vibrancy and freshness to the dish ... grapes are a deep purple ... A fork and knife are neatly placed beside the plate, indicating a formal dining setting.  
**Paraphrased Question:** What type of fruit is cut in half and darker than the other fruit in the salad?  
**Reasoning:**  
The image shows a plate of food containing a salad ... The salad includes grapes, which are cut up and darker than the other fruits. The grapes are a deep purple color that is darker. The answer to the question "What type of fruit is cut in half and darker than the other fruit in the salad?" is "grapes."  
**Final Answer:** grapes. ✔️

Figure 10. Performance of VIKSeR and baselines on a visual reasoning task involving short-answer questions.



**Question:**  
What is the white substance on top of the cupcakes?

**Answer:**  
icing.

**Reasoning:** Llava 1.5 - CoT  
A person's hand pointing at two cupcakes with white frosting and red decorations. The frosting is white, and the decorations are red, which indicates that the cupcakes are likely vanilla flavored with strawberry toppings.

**Final Answer:** The white substance is frosting. ❌

**Reasoning:** Qwen2.5 - CoT  
The image shows a close-up of a person's hand decorating cupcakes with what appears to be a white frosting or cream. The cupcakes have a light-colored base, possibly vanilla, and are topped with a dollop of white frosting, which could be buttercream or whipped cream.  
**Final Answer:** buttercream or whipped cream. ❌

**Reasoning:** Blip2-Flan-t5-xxl - CoT  
The image shows a cupcakes are topped with a layer of white substance. This substance has a smooth appearance, typically used to decorate cakes and enhance flavor. Based on the usage and appearance, the white substance on top of the cupcakes is frosting.  
**Final Answer:** frosting. ❌

**Reasoning:** GPT-4o-mini  
The white substance on top of the cupcakes appears to be frosting, likely buttercream frosting, which is commonly used for decorating cupcakes. It's creamy and can be piped into various shapes, as seen in the image. Buttercream frosting is typically made from butter, powdered sugar, and vanilla extract.  
**Final Answer:** frosting. ❌

**Caption:** ViKSeR (Ours)  
A hand is skillfully decorating a cupcake with frosting and a raspberry ... **The frosting is the icing** ... The cupcake is placed on a countertop, surrounded by baking ingredients, emphasizing the creative process in a kitchen setting ... The hand's action of pointing at the raspberry and applying the frosting highlights the attention to detail ...  
**Paraphrased Question:** What type of fruit is cut in half and darker than the other fruit in the salad?  
**Reasoning:**  
In the image, a person's hand is skillfully decorating a cupcake with frosting and a raspberry. The frosting is the icing, which is commonly used to decorate cupcakes. Therefore, the answer to the question "What is the white frosting on the cupcakes made from?" is "icing."  
**Final Answer:** icing. ✔️

Figure 11. Performance of ViKSeR and baselines on a visual reasoning task involving short-answer questions.



**Question:**  
Is the man on the left platform going to board the train?

**Answer:**  
No.

**Reasoning:** Llava 1.5 - CoT

The image shows a train on the tracks with people standing on the platform. One of the people is a man who is standing on the left platform. The train is approaching the station, and the man is likely waiting to board the train.

**Final Answer:** Yes. ✗

**Reasoning:** Qwen2.5 - CoT

The image depicts a train station with a train arriving at the platform. The person on the left platform appears to be standing near the edge, possibly waiting for the train to stop before boarding. However, there is no clear indication that this person is actively boarding the train at this moment.

**Final Answer:** uncertain. ✗

**Reasoning:** Blip2-Flan-t5-xxl - CoT

**Reasoning:**

The image shows a man standing on the left platform, with a train located on the right platform. The position relationship between the train and the man is clear, standing on different platforms.

**Final Answer:** The man is on the left platform and the train is on the right platform. ✗

**Reasoning:** GPT-4o-mini

It's difficult to determine whether the man is going to board the train based on the image alone. The man's body language, position relative to the train would provide more context. If he is near the edge of the platform and facing the train, he may be preparing to board. However without additional information, it's uncertain.

**Final Answer:** uncertain. ✗

**Caption:**

**ViKSeR (Ours)**

A blue and yellow train travels down the right side of the tracks, approaching a train station ... A man is on the other side of the tracks ... The train is carrying passengers on the platform, who are waiting to board or disembark ... The train tracks, located adjacent to the station, guide the train's movement and direction.

**Paraphrased Question:** Is the man on the left platform going to board the train on the right side of the tracks?

**Reasoning:**

The man is standing on the left platform, and the train is on the right platform. The train is moving, and the man is not boarding it. The man is far away from the other train, and he's on the other side of the tracks. The answer to the question "Is the man on the left platform going to board the train on the right side of the tracks" is "no."

**Final Answer:** No. ✓

Figure 12. Performance of ViKSeR and baselines on a visual reasoning task involving a true/false question.



**Question:**  
Why would you use this suitcase?

**Answer:**  
travel.

**Reasoning:** Llava 1.5 - CoT

The image shows a suitcase filled with various items such as bottles, a backpack, and a teddy bear. The suitcase is open and placed on the floor. The presence of these items suggests that the suitcase is being used for transporting belongings.

**Final Answer:** transporting belongings. ❌

**Reasoning:** Qwen2.5 - CoT

The image shows an open suitcase filled with various items such as toiletries, medications, and possibly some clothing, all of which appear to be personal belongings. The word "baggage" is prominently displayed, which indicates that the suitcase is used for carrying personal belongings.

**Final Answer:** carrying personal belongings. ❌

**Reasoning:** Blip2-Flan-t5-xxl - CoT

**Reasoning:**

The image shows an open suitcase filled with various things, including toiletries, medications, and some clothes. It is obvious that this suitcase is very large and can hold a lot of things.

**Final Answer:** this suitcase can hold a lot of things. ❌

**Reasoning:** GPT-4o-mini

This suitcase appears to be packed with a variety of items, suggesting it may be used for a long trip or vacation. The presence of toiletries, grooming supplies, and other personal items indicates that the owner is likely preparing for travel abroad or a family visit ... Overall, the suitcase seems suited for travel.

**Final Answer:** travel. ✅

**Caption:**

**ViKSeR (Ours)**

A suitcase is opened and filled with various toiletries and personal items for daily use, reflecting the process of **packing for travel** ... The suitcase is positioned on the floor, surrounded by **other travel accessories** such as a backpack ... A bag placed next to the suitcase indicates that it is being used to store or transport other items.

**Paraphrased Question:** What is the purpose of this suitcase, which is filled with items necessary for daily use?

**Reasoning:**

The image shows a suitcase filled with various toiletries and personal items, indicating that it is packed for travel ... The presence of the suitcase and its contents suggest that the purpose of this suitcase is for daily use during travel.

**Incorrect Answer:** daily use. ❌

**Self-Reflection:** In the previous trial, I failed to address the question as I answer the phrase "daily use," which may not have been clear enough in context. The purpose of the suitcase is to pack for travel, so I will adjust the reasoning to focus more directly on the travel aspect.

**New Reasoning:**

The image shows an open suitcase packed with toiletries and personal items typically associated with travel ... The arrangement of items such as toiletries suggests preparation for travel ...

**Final Answer:** travel. ✅

Figure 13. Performance of VIKSER and baselines on a visual reasoning task involving short-answer questions.